

---

## Simulation of suspension of solids in a liquid in a mixing tank using SPH and comparison with physical modelling experiments

---

Mahesh Prakash\*, Paul W. Cleary and Joseph Ha

CSIRO Mathematical and Information Sciences, Clayton, VIC 3169, Australia  
E-mail: Mahesh.Prakash@csiro.au

\*Corresponding author

Mohammed Nabil Noui-Mehidi and Hugh M. Blackburn

CSIRO Manufacturing and Infrastructure Technology, Highett, VIC 3190, Australia

Geoff Brooks

CSIRO Minerals, Clayton, VIC 3169, Australia

**Abstract:** This paper demonstrates the use of Smoothed Particle Hydrodynamics (SPH) to simulate a suspension of solids in a liquid mixing tank when the solids are large and have a high loading in comparison with the liquid in the tank. The simulations are validated by comparing the results with physical modelling experiments that shows a relationship between the submergence criterion of the solids and the impeller speed. The experiments were conducted using water as the fluid and cylindrical blocks of wood with a specific gravity of 0.5 with near identical conditions being used for the simulations.

**Keywords:** smoothed particle hydrodynamic modelling; SPH; solid-liquid mixing; pellet submergence; impeller speed; solids loading.

**Reference** to this paper should be made as follows: Prakash, M., Cleary, P.W., Ha, J., Noui-Mehidi, M.N., Blackburn, H.M. and Brooks, G. (2007) 'Simulation of suspension of solids in a liquid in a mixing tank using SPH and comparison with physical modelling experiments', *Progress in Computational Fluid Dynamics*, Vol. 7, Nos. 2/3/4, pp.91–100.

**Biographical notes:** Mahesh Prakash is a Research Scientist at CSIRO Mathematical and Information Sciences, Australia. His research interests include application of grid-free methods to industrial flow problems, turbulence modelling using Smoothed Particle Hydrodynamics (SPH) and non-Newtonian flow modelling using SPH.

Paul Cleary is a Research Scientist at CSIRO Mathematical and Information Sciences, Australia and Leader of the Computational Fluid Dynamics Group. His research interests include development of the grid-free methods of Smoothed Particle Hydrodynamics and Discrete Element Modelling for industrial fluid and particle flow problems.

Joseph Ha is a Research Scientist at CSIRO Mathematical and Information Sciences, Australia. His research interests include the computational aspects of SPH and the application of SPH to solve industrial problems.

Mohamed Nabil Noui-Mehidi is a Research Scientist in the Fluids Engineering Group at CSIRO Manufacturing and Infrastructure Technology. His research area is related to multiphase fluid dynamics applied to the mineral and oil and gas industries.

Hugh Blackburn is a Senior Research Scientist in the Fluids Engineering Group at CSIRO Manufacturing and Infrastructure Technology. His research interests include application of high order numerical methods to direct and large eddy simulation of industrial and biomedical turbulent flows, and the development and application of new flow stability analysis methods.

Geoffrey Brooks is a Professor at Swinburne University, Melbourne, Australia. Previously, he was a Principal Research Scientist at CSIRO, Australia, Associate Professor of Materials Science and Engineering at McMaster University and a Senior Lecturer at the University of Wollongong in Materials Engineering. He has a PhD in Extractive Metallurgy from the University of Melbourne. His research is focused on understanding the kinetics of high temperature processes.

## 1 Introduction

In many industrial systems such as crystallisation, liquid-solid reactions, reactions with solid catalysts and leaching, there is a need to suspend solids in the liquid using some form of mixing (Baldi et al., 1981; Yamazaki et al., 1991). If the solid particle size and the loading are small in comparison with the volume of the liquid in the mixing vessel then one can effectively use continuum two-phase models for the purpose of simulation (see Ling et al., 2003 as one of many examples). However, if the solids are physically larger, with length scales that are not particularly small when compared to the size of the mixing tank and the impeller, or have high solids loadings so that they cannot be considered as dilute, then they need to be modelled individually and the fluid flow around these particles needs to be adequately resolved. Traditional grid based methods find it prohibitively difficult to describe such flows due to the complicated grid transformations that need to be carried out for such computations.

SPH is a Lagrangian (grid-free) simulation method that has been used extensively to model fluid flows with heat transfer for different applications such as high pressure die casting (Cleary and Ha, 2003), ingot casting of aluminium (Cleary et al., 2004), modelling of bio-pumps (Gomme et al., 2006), simulation of broken ice-fields (Gutfraind and Savage, 1997) and flow through porous media (Zhu and Fox, 2002). Due to its grid-free nature it has the following advantages over other more conventional CFD methods:

- free surface flows can be handled automatically and accurately
- solid/fluid interactions with complicated motions of the solid parts can be simulated with few additional computational penalties
- complicated physics can be added easily (examples include non-Newtonian rheology, solidification, freezing, solid stress and history dependence of fluid variables).

Due to these inherent advantages it was decided to extend the SPH method to include solid pellets in a liquid for various applications. The present approach differs from the technique used by Potapov et al. (2001) in that the latter uses DEM particles to represent the solids and SPH to represent the liquid phase, whereas here, we use a collection of SPH particles to represent the solid and represent the fluid in the usual way using SPH fluid particles.

The applicability of the present method is demonstrated in this paper by firstly simulating the acceleration of a single solid particle and verifying the solution by comparison with analytical results. Secondly, simulations of 3D mixing and submergence in a liquid filled cylindrical tank driven by a central impeller and containing buoyant cylindrical particles are validated by comparison with physical experiments. This shows a relation between the submergence criterion and parameters such as size of solids, solids loading and impeller speed. The experiments were conducted using

water as the fluid and cylindrical blocks of wood with a specific gravity of 0.5 as the solids, with identical conditions being used for the simulations.

## 2 SPH methodology

A brief summary of the SPH method is presented here. For more comprehensive details refer to Monaghan (1992). The interpolated value of a function  $A$  at any position  $\mathbf{r}$  can be expressed using SPH smoothing as:

$$A(\mathbf{r}) = \sum_b m_b \frac{A_b}{\rho_b} W(\mathbf{r} - \mathbf{r}_b, h) \quad (1)$$

where  $m_b$  and  $\mathbf{r}_b$  are the mass and density of particle  $b$  and the sum is over all particles  $b$  within a radius  $2h$  of  $\mathbf{r}$ . Here  $W(\mathbf{r}, h)$  is a  $C^2$  spline based interpolation or smoothing kernel with radius  $2h$  that approximates the shape of a Gaussian function. The gradient of the function  $A$  is given by differentiating the interpolation Equation (1) to give:

$$\nabla A(\mathbf{r}) = \sum_b m_b \frac{A_b}{\rho_b} \nabla W(\mathbf{r} - \mathbf{r}_b, h). \quad (2)$$

Using these interpolation formulae and suitable finite difference approximations for second order derivatives, one is able to convert parabolic partial differential equations into ordinary differential equations for the motion of the particles and the rates of change of their properties.

From Monaghan (1992), our preferred form of the SPH continuity equation is:

$$\frac{d\rho_a}{dt} = \sum_b m_b (\mathbf{v}_a - \mathbf{v}_b) \cdot \nabla W_{ab} \quad (3)$$

where  $\rho_a$  is the density of particle  $a$  with velocity  $\mathbf{v}_a$  and  $m_b$  is the mass of particle  $b$ . We denote the position vector from particle  $b$  to particle  $a$  by  $\mathbf{r}_{ab} = \mathbf{r}_a - \mathbf{r}_b$  and let  $W_{ab} = W(\mathbf{r}_{ab}, h)$  be the interpolation kernel with smoothing length  $h$  evaluated for the distance  $|\mathbf{r}_{ab}|$ . This form of the continuity equation is the Galilean invariant (since the positions and velocities appear only as differences), has good numerical conservation properties and is not affected by free surfaces or density discontinuities.

The momentum equation then becomes the acceleration for each particle:

$$\begin{aligned} & \frac{d\mathbf{v}_a}{dt} \\ &= \mathbf{g} - \sum_b m_b \left[ \frac{P_b}{\rho_b^2} + \frac{P_a}{\rho_a^2} - \frac{\xi}{\rho_a \rho_b} \frac{4\mu_a \mu_b}{(\mu_a + \mu_b)} \frac{\mathbf{v}_{ab} \mathbf{r}_{ab}}{r_{ab}^2 + \eta^2} \right] \nabla_a W_{ab} \end{aligned} \quad (4)$$

where  $P_a$  and  $\mu_a$  are pressure and viscosity of particle  $a$  and  $\mathbf{v}_{ab} = \mathbf{v}_a - \mathbf{v}_b$ . Here  $\xi$  is a factor associated with the viscous term (Cleary, 1996),  $\eta$  is a small parameter used to smooth out the singularity at  $\mathbf{r}_{ab} = 0$  and  $\mathbf{g}$  is the gravity vector. Other equations such as the energy equation can be derived in a similar manner (Cleary and Prakash, 2004). Since the SPH method used here is quasi-compressible one needs to

use an equation of state, giving the relationship between particle density and fluid pressure. A suitable one is:

$$P = P_0 \left[ \left( \frac{\rho}{\rho_0} \right)^\gamma - 1 \right] \quad (5)$$

where  $P_0$  is the magnitude of the pressure and  $\rho_0$  is the reference density. For water or liquid metals we use  $\gamma=7$ . This pressure is then used in the SPH momentum Equation (4) to give the particle motion.

SPH resolves all length scales of the flow above the resolution length, much like a Large Eddy simulation. However, there is no formal turbulence modelling since the present SPH does not have a sub-grid scale model.

#### Governing equation for solid pellet motion

SPH is well suited to represent solid particles advected in a liquid flow. The lack of a mesh allows the fluid to flow very naturally around the solids. Each pellet is constructed from an array of SPH particles with physical properties matching those of the pellet. The continuity and momentum Equations (3) and (4) are used to predict the forces between each fluid and solid particle in the usual way. The pellets are modelled as rigid bodies, so no forces are calculated between the SPH particles within each pellet. The continuity equation solution leads to variations in the density of the solid particles, which via the equation of state (Eq. 5), provide a prediction of the fluid pressure distribution on the surface of the pellet due to its interaction with the fluid. After the spatially varying fluid forces on the surface of the solid pellet are calculated using Equation (4) for each of its constituent SPH particles, the net force and torque on the pellet are calculated. The rigid body equations of motion for the pellet position and orientation are then integrated using second order accurate time integration of the same form as used in the integration of the fluid SPH particles.

### 3 Motion of single pellet

As a preliminary test to evaluate the implementation of solid pellet motion, single pellet SPH simulations were performed under constant acceleration in the absence of fluid. The results are compared with analytical solutions.

In Figure 1 the SPH prediction of the motion of a single pellet subjected to constant acceleration in the  $y$  direction is compared with the analytical solution. The SPH solution is given by crosses and the analytical solution by the dotted line. The SPH solution matches the analytic solution very closely, with the solid pellet accelerating in the  $-y$  direction. Figure 2 compares the analytical and SPH solution for a pellet accelerating in the positive  $x$  direction. Here again the exact and the SPH solution are very closely matched. Finally Figure 3 shows a comparison between the SPH and analytical solution for a pellet moving with constant acceleration in the  $y=x$  direction. Here, the vertical axis represents the distance travelled along the  $x$  and  $y$  directions. Again almost an exact match exists between the analytical and SPH results for both the  $x$  and  $y$  distance travelled by

the pellet. These results indicate that SPH pellet integration predicts the motion of single pellets in the absence of fluid flow very accurately.

**Figure 1** Comparison between SPH and analytical solutions for constant acceleration in  $-y$  direction

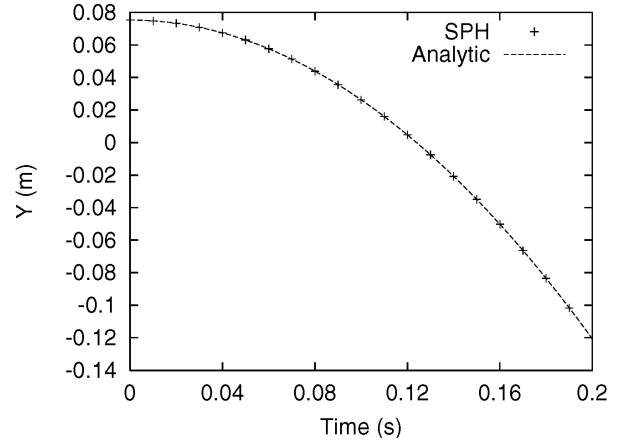


**Figure 2** Comparison between SPH and analytical solutions for constant acceleration in  $x$  direction

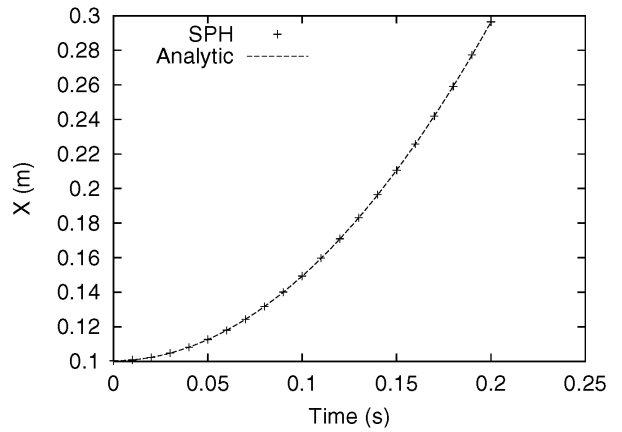
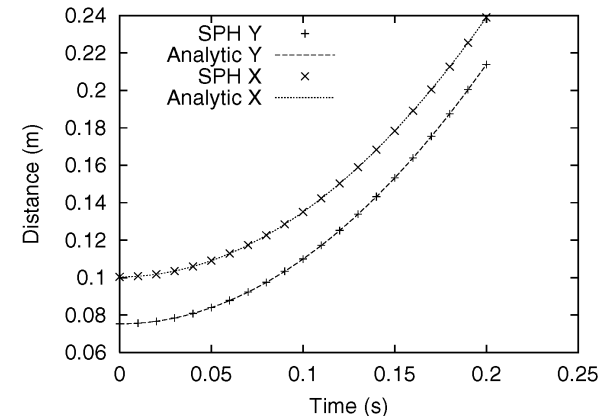


**Figure 3** Comparison between SPH and analytical solutions for constant acceleration in  $y=x$  direction



### 4 Experimental set-up for 3D mixer

Having established that the solid pellet implementation gives the correct kinematic motion, a set of experiments were performed for validating simulations:

- having solid pellets interacting with each other
- with pellets interacting with the surrounding fluid
- under varying degrees of external forces acting on the fluid and pellets.

This was done by using experimental data for a large impeller stirred mixing tank. The mixer experimental setup consisted of a cylindrical vessel with 1.0 m diameter constructed from acrylic with a single baffle, as shown in Figure 4. The baffle forces the vortex generated by the impeller motion to be off-centre and was expected to aid the submergence of pellets by the fluid (Joosten et al., 1977). A four bladed downward-pumping type impeller as shown in Figure 5 is used in the experiments to generate a circulatory and vortical flow structure. The impeller speed is varied from 78 rpm to about 220 rpm, imparting varying degrees of external force on the fluid and solids. The tank is filled to a height of 1 m by water. The pellets were made from cylindrical sections of wood with a specific gravity of 0.5. Pellet dimensions of 16 mm (diameter) × 22.5 mm (height) and 25 mm (diameter) × 35 (height) mm were used for the experiments, giving pellet aspect ratios of 1.4. Pellet loadings of 1.5 kg and 4 kg were used for the 16 mm pellets and a loading of 1.5 kg was used for the 25 mm pellets. Visual observation was used to determine the approximate minimum critical impeller speeds for complete submergence of pellets in the fluid for different pellet sizes and loadings (Noui-Mehidi et al., 2005).

Figure 4 Schematic of the experimental mixer set-up

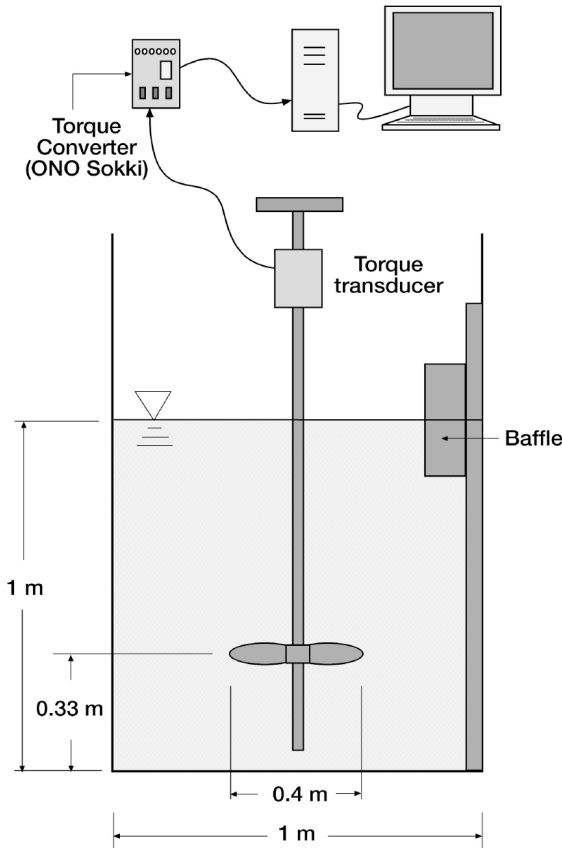
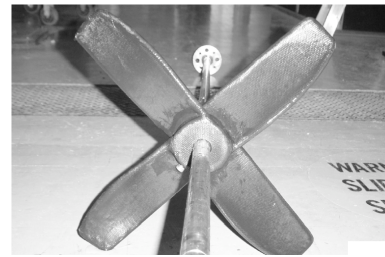
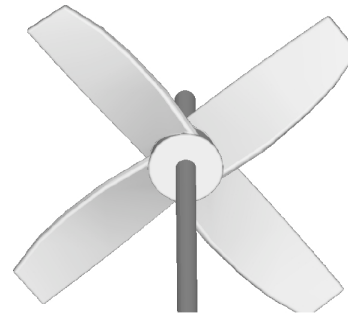


Figure 5 Four bladed downward pumping impeller used for suspending solid pellets: (a) physical and (b) model



(a)



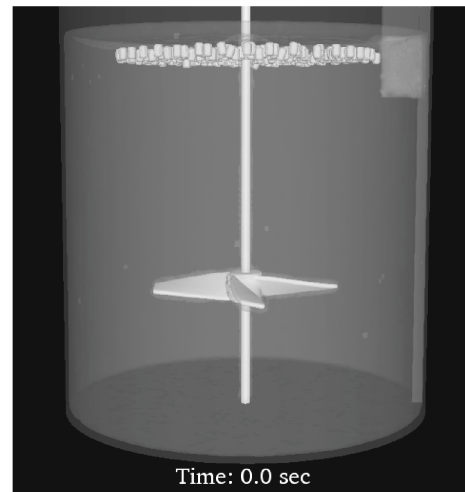
(b)

### 5 Simulation set-up for 3D mixer

Figure 5(b) shows a CAD model of the impeller that was constructed based on the experimental impeller design. The impeller, shaft and tank were meshed at a uniform resolution of 4.0 mm using a commercial meshing package. This mesh was converted into SPH particles using an in-house pre-processor.

Figure 6 shows the complete SPH setup, including the tank with the single baffle (semi-transparent), the impeller with the impeller shaft at the centre of the tank (opaque), the fluid is filled to a height of 1.0 m (and is semi-transparent) with pellets (opaque) floating on top of the fluid.

Figure 6 Initial 3D setup for SPH simulation of the mixer, including the pellets located at the top. Here the pellet diameter is 16 mm and the pellet loading is 1.5 kg



Variable SPH particle sizes were used for different parts of the simulations due to two competing requirements:

- need to increase the speed of simulations
- maintenance of adequate resolution for different sections of the geometry, pellets and fluid.

Since the impeller thickness was around 12.0 mm a particle size of 4.0 mm was used for the impeller as well as the shaft, tank and baffle. A fine resolution for the boundary does not lead to a large increase in computational time in SPH. A SPH particle size of 8.0 mm was used in order to resolve the solid pellets adequately. Around 28 SPH particles were required to construct each pellet. A coarser particle size of 16.0 mm was used for the fluid. These resolutions required approximately 380,000 boundary particles, 170,000 fluid particles and between 6000 and 16000 pellet particles depending on the pellet loading.

The set of simulations described in this paper consists of four different impeller speeds of 53, 150, 180 and 200 rpm for a pellet loading of 1.5 kg and a pellet diameter of 16 mm. For this case there were a total of 210 pellets in the simulation.

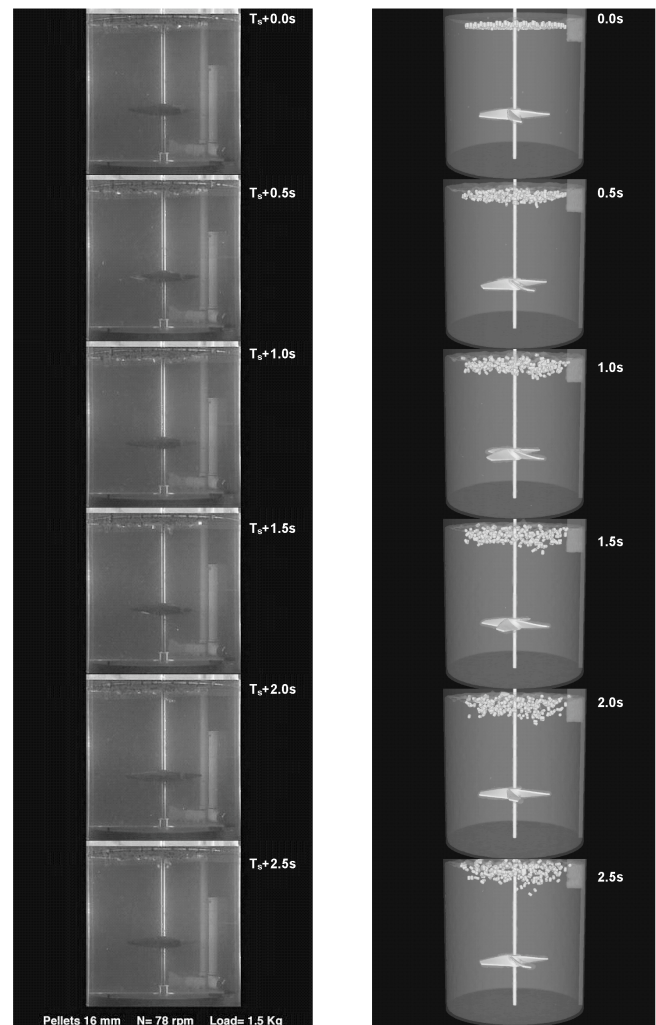
## 6 Experimental and SPH visualisations

In the experiments, the impeller starts from rest and accelerates for some time until it reaches a final steady speed. Conversely, in the simulations, the impeller starts at the specified speed in order to shorten the simulation time required. A suitable point in the experimental start up phase, that is most reasonably equivalent to the simulation start, is chosen as the corresponding experimental start time in order to correctly synchronise the two flows.

### 6.1 Comparison for low impeller speed

In the experiments the power required to submerge pellets showed sensitivity to the pellet size only after an impeller speed of about 140 rpm (Noui-Mehidi et al., 2005). This means that impeller speeds significantly below this value can reasonably safely be considered to show similar behaviour. Results can thus be compared for such cases. Figure 7 compares results at a low impeller speed; the experimental result was 78 rpm and the simulation was 53 rpm for 16 mm pellets at a loading of 1.5 kg. At the start time, both simulation and experiment have the pellets floating just below the surface of the fluid. The fluid free surface is predicted to be reasonably flat and is done automatically and dynamically by SPH due to its grid-free nature.

**Figure 7** Comparison between experiment (78 rpm) and simulation (53 rpm), 16 mm pellet, 1.5 kg for low impeller speed



At 0.5 s, the pellets in the experiment maintain their overall position. The pellets in the simulation have begun to sink slightly into the fluid. At 1.0 s the experimental data show little evidence of downward motion by the pellets, whilst in the simulation the pellets have moved slightly further down into the fluid.

At 1.5 s, the position of the pellets in the simulation does not appear to have changed, indicating that at this impeller speed the pellet distribution has reached equilibrium and are not on average submerged further down into the fluid. At the corresponding time in the experimental data, there is now evidence of some downward movement of the pellets. This is seen clearly at 2.0 s where 3–4 pellets have moved down into the fluid from close to the impeller shaft. At 2.0 s, the simulation shows no appreciable change

from 1.5 s except perhaps for a slight clustering of the pellets close to the centre of the tank as a result of the central vortex created by the impeller motion. At 2.5 s, in both the experiment and simulation, the pellets appear to have started to slightly move upwards, indicating that these impeller speeds are insufficient to maintain submergence of the pellets over sustained periods of time.

In summary, for low impeller speeds:

- The pellets in the experimental data show slightly less downward motion compared to the simulation.
- The experimental and simulated pellets show that once a steady flow state is reached it is not sufficiently strong to submerge the pellets into the fluid. Pellets that had started to sink rise back to the surface at these low impeller speeds.

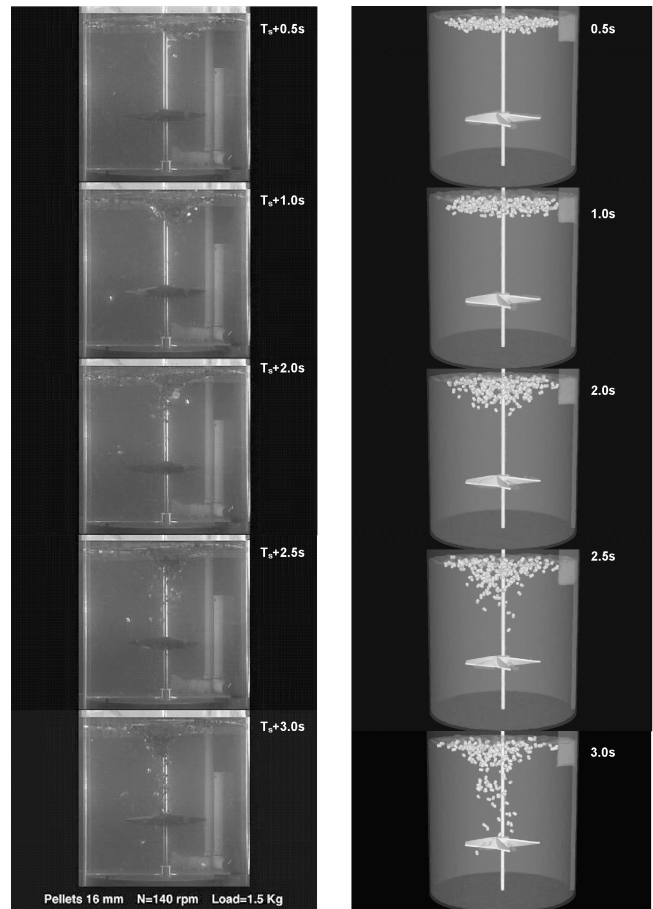
## 6.2 Comparison for medium impeller speed

Figure 8 shows a comparison between the experimental data (at 140 rpm) and the simulation (at 150 rpm), which are fairly closely matched at medium strength impeller speeds. The initial frame (from the start time) is the same as shown in Figure 7 and is therefore not shown here. At 0.5 s, in the experiment one can see a slightly off-centre downward vortex of pellets. In the simulation, the pellets have just started moving downwards and are accumulating closer to the centre of the tank as a result of the central vortex created by the impeller motion.

At 1.0 s the pellets in both sets of data show some further downward movement, with pellets close to the impeller shaft in the experimental data showing a slightly lower position to those seen in the simulation, which are moving slower but more uniformly in comparison. At 1.0 s, the pellets migrate towards the core of the vortex but since the flow pattern in the fluid is still developing, there is not much downward motion of the pellets either in the experiment or in the simulation.

At 2.0 s and 2.5 s, the experiment and simulation are more closely matched. The pellets are now experiencing almost the full force of the impeller motion. The central vortex has now started submerging pellets (about 8 or 9) to such an extent that they are near the impeller blades (see frame at 2.5 s for example). Here, the simulation is able to quite accurately capture the location of the lowest pellets. In the experimental data, at 2.5 s there are a significant number of pellets still floating close to the surface of the fluid, and this is accurately predicted in the simulation.

**Figure 8** Comparison between experiment (140 rpm) and simulation (150 rpm), 16 mm pellet, 1.5 kg for medium impeller speed



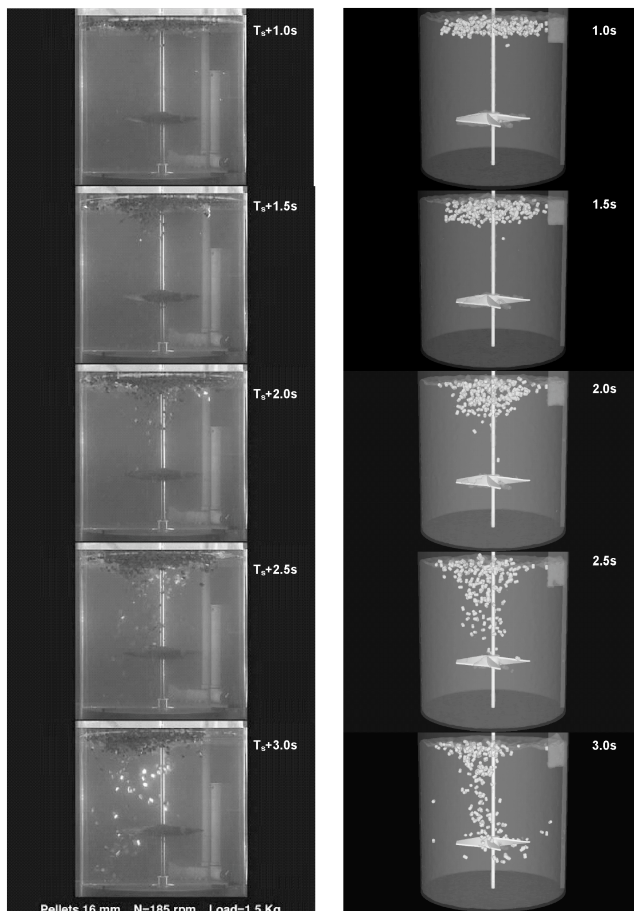
At 3.0 s the fluid flow pattern is fully established and the pellets that were close to the impeller blades have now reached the blades and are circulating with the fluid motion. This impeller induced recirculation of the fluid, and the corresponding pellet motion, is well predicted by the simulation. This can especially be seen from the accurate prediction of the conical structure of the group of pellets that are drawn down from close to the impeller shaft due to the impeller motion.

At 3.0 s there are still a substantial number of pellets located close to the fluid free surface. The simulation accurately predicts this and demonstrates that although the flow pattern is now fully established the impeller force generated at such intermediate speeds (140–150 rpm) is still insufficient to submerge all pellets.

### 6.3 Comparison for high impeller speeds

Figure 9 compares experiment (185 rpm) and simulation (180 rpm) at high impeller speeds. At 1.0 s, in both the experimental and simulation data, the pellets have begun to be pulled down into the fluid. At 1.5 s in the experimental data, the pellet layer on top has broken down and the formation of a regular vortical structure as observed in the medium impeller speed case is absent. The pellets have started migrating towards the impeller shaft. In the simulation data one can see a similar breaking down of the pellet layer on top, albeit to a lesser extent.

**Figure 9** Comparison between experiment (185 rpm) and simulation (180 rpm), 16 mm pellet, 1.5 kg for high impeller speed



At 2.0 s in the experiment, the flow pattern has become more established and a somewhat fragmented central stream of pellets can be seen descending towards the impeller blades, with a few pellets becoming quite close to the impeller blades. A very similar pellet flow structure can be seen in the simulation at 2.0 s.

At 2.5 s, the pellet motion has become quite chaotic, with almost half of the pellets moving closer to the impeller blades. The suction resulting from the impeller motion is much more effective here compared to the medium speed impeller case. The simulation predicts the increased level of pellet submergence as well as the number of pellets being submerged. At this point one can begin to see a significant

reduction in the amount of pellets occupying the surface of the fluid in the experiment and simulation.

At 3.0 s, the experimental data for high impeller speeds shows that pellets that have been submerged in the fluid remain beneath the surface whilst further pellets are pushed downwards into the fluid. Many of the pellets have started to strike the impeller blades and are following a recirculation pattern within the fluid. A similar observation can be made from the simulation data, with pellets showing strong chaotic behaviour within the fluid as they hit the impeller blades and begin to recirculate.

One minor difference between the experiment and simulation is the location of the stream of pellets as they become submerged. In the experiment this seems to be to the left of the impeller shaft, (see the frames on the left at 2.5 s and 3.0 s), whilst in the simulation this stream of pellets is located slightly to the right of centre of the impeller shaft. Other than this, the overall flow structure is similar in both sets of data.

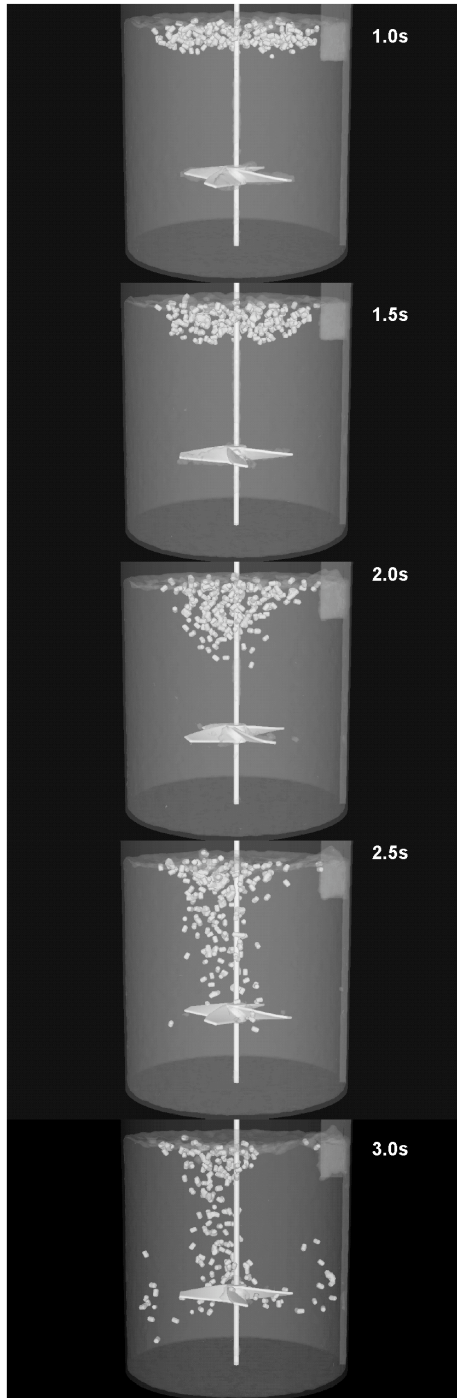
A visual observation of the fluid free surface in the experiments (Noui-Mehidi et al., 2005), found that the minimum critical impeller speed for complete submergence of 16 mm pellets with a 1.5 kg loading is 180 rpm. At 3.0 s, large sections of the fluid free surface are cleared of pellets in the simulation. This was not apparent in the 150 rpm simulation discussed earlier, indicating that at 180 rpm one is approaching the critical submergence speed for this pellet size and loading.

In order to further explore the behaviour of pellets at higher impeller speed, a simulation was run at 200 rpm, with the flow predictions shown in Figure 10. The resulting flow shows a similar structure to that observed in the 180 rpm case. The pellets move close to the centre of the tank at 1.0 s and 1.5 s as a result of impeller motion. At 2.0 s they start moving down into the fluid. The motion becomes more chaotic as time progresses and as the recirculating flow pattern becomes fully established at 2.5 s, a significant proportion of the pellets have moved down. At 3.0 s one can see pellets being recirculated within the fluid, as well as a clear fluid free surface, showing complete pellet submergence.

From these observations for the high impeller speeds one can conclude qualitatively that:

- The simulations predict the critical impeller speed for complete pellet submergence quite well. The experiment (Noui-Mehidi et al., 2005) showed that this is around 180 rpm through a visual observation of the fluid free surface. In the simulation, large sections of the fluid free surface first become clear at 180 rpm, with many pellets becoming submerged and recirculating within the fluid.
- The submergence and recirculation pattern for the 200 rpm simulation are similar to the 180 rpm one. This further emphasises that the critical impeller speed for submergence predicted by the simulation is around 180 rpm.

**Figure 10** Simulation 200 rpm, 16 mm pellet and 1.5 kg

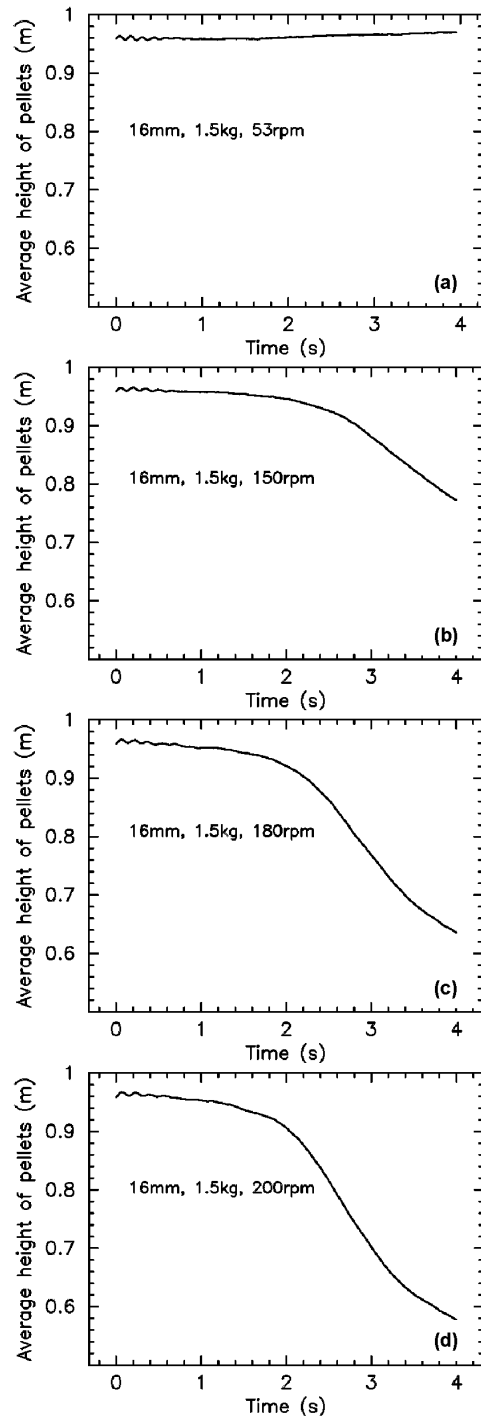


**7 Average height of pellets**

In order to quantitatively assess the degree of submergence of the pellets at different impeller speeds the average height of all pellets above the base of the tank was tracked over time for each simulation. Figure 11 shows the average height of the pellets as a function of time for the speeds 53, 150, 180 and 200 rpm. In each case, the vertical axis represents the average pellet height in metres. At 53 rpm the average height starts at about 0.96 m (with the fluid

level at 1.0 m) and remains steady at this level after 4.0 s or about 3.5 impeller revolutions.

**Figure 11** Simulated average height of pellets with time for: (a) 53 rpm; (b) 150 rpm; (c) 180 rpm and (d) 200 rpm



At 150 rpm, the average fluid height drops to 0.95 m after 1.0 s or 2.5 revolutions and about 0.94 m after 2.0 s or 5 impeller revolutions. After 2.0 s, the rate of submergence increases as the recirculating fluid flow pattern becomes fully developed. At 3.0 s (7.5 revolutions) the average pellet height has reached 0.89 m with a further reduction to 0.77 m at 4.0 s (ten revolutions). This means that at 150 rpm the

pellets have, on average, submerged by 19.8% after ten impeller revolutions.

At 180 rpm, the average pellet height has dropped to about 0.95 m at 1.0 s (3 impeller revolutions) and 0.93 m at 2.0 s (six impeller revolutions). This means that in the initial stages of the simulation the pellet height does not change significantly between the 150 rpm and 180 rpm cases, since the recirculating flow pattern is still not established at this early time. By 3.0 s (nine revolutions) there is a sharp drop in the average pellet height to 0.77 m and a further drop to 0.62 m at 4.0 s (12 revolutions). The pellets have submerged, on average, by 35% after 4.0 s or 12 impeller revolutions and can be expected to be increasingly submerged with time.

At 200 rpm, the average pellet height does not change significantly for the first 2.0 s of simulation as the fluid flow pattern is still developing. It then drops sharply to 0.7 m at 3.0 s or 10 revolutions, and further to 0.57 m at 4.0 s or 13.3 revolutions. In this case, the pellets have submerged, on an average, by 41% after 4.0 s or 13.3 revolutions.

The simulations support the experimental hypothesis that a critical impeller speed exists at about 180 rpm. This is the lowest speed that leads to substantial and sustained submergence of 16 mm pellets at a loading of 1.5 kg.

## 8 Conclusions

This paper presents a comparison between experiments and 3D SPH simulations for a mixing tank driven by a central impeller with buoyant solid pellets in a fluid. The SPH simulations were carried out for four different impeller speeds of 53 rpm (low speed), 150 rpm (medium speed), 180 rpm and 200 rpm (high speed) with 16 mm diameter pellets and at a loading of 1.5 kg. The experimental and simulation results showed that:

- At low impeller speeds the pellets tend to remain at the surface of the fluid in the experiment and simulation even after a long duration.
- At medium impeller speeds only some pellets are dragged down far from the free surface by the vortical flow pattern generated by the impeller motion. The extent of pellet submergence in the fluid is predicted very well by the simulations. There is a substantial amount of pellets still floating close to the free surface at this speed, even after ten impeller revolutions. This is observed in both the experiment and the simulation. One can reasonably conclude that these moderate impeller speeds will never substantially submerge the pellets.
- At high impeller speeds, almost all pellets move down towards the impeller blades and start recirculating within the fluid once the flow pattern is established. This phenomenon is predicted extremely well by the simulations. The fluid free surface becomes fairly clear of pellets in the experiment at 185 rpm and SPH predictions at both 180 rpm and 200 rpm. This indicates that both in the experiment and simulation, the critical speed for complete pellet submergence is around 180 rpm for a pellet size of 16 mm and loading of 1.5 kg.

These conclusions are confirmed by looking at quantitative measures such as the average height of the pellets in the tank as a function of time for the different impeller speeds.

## Acknowledgements

The work described in this paper was conducted in the Light Metals Flagship, a National Research Flagship initiated by CSIRO.

## References

- Baldi, G., Conti, R. and Gianetto, A. (1981) 'Concentration profiles for solids suspended in a continuous agitated reactor', *A. I. Ch. E. J.*, Vol. 27, pp.1017–1020.
- Cleary, P. (1996) *New Implementation of Viscosity: Tests with Couette Flows*, SPH Technical Note 8, CSIRO DMS, Technical Report DMS – C 96/32.
- Cleary, P., Grandfield, J., Prakash, M., Ha, J., Sinnott, M. and Nguyen, T. (2004) 'Modelling of casting systems using smoothed particle hydrodynamics', *J. Metals*, Vol. 3, pp.67–70.
- Cleary, P.W. and Ha, J. (2003) 'Three-dimensional SPH simulations of light metal components', *J. Light Metals*, Vols. 2–3, pp.169–183.
- Cleary, P.W. and Prakash, M. (2004) 'Discrete element modelling and smooth particle hydrodynamics: potential in the environmental sciences', *Phil. Trans. R. Soc. London A*, Vol. 362, pp.2003–2030.
- Gomme, P.T., Prakash, M., Hunt, B., Stokes, N., Cleary, P., Tatford, O.C. and Bertolini, J. (2006) 'Effect of lobe pumping on human albumin: development of a lobe pump simulator using smoothed particle hydrodynamics', *Biotechnology and Applied Biochemistry*, Vol. 43, pp.113–120.
- Gutfraind, R. and Savage, S.B. (1997) 'Smoothed particle hydrodynamics for the simulation of broken-ice fields: Mohr–Coulomb-type rheology and frictional boundary conditions', *J. Comput. Physics*, Vol. 134, pp.203–215.
- Joosten, G.E.H., Schilder, J.G.M. and Broere, A.M. (1977) 'The suspension of floating solids in stirred vessels', *Trans IChemE*, Vol. 55, pp.220–222.

- Ling, J., Skudarnov, P.V., Lin, C.X. and Ebadian, M.A. (2003) 'Numerical investigations of liquid-solid slurry flows in a fully developed turbulent flow region', *Int. Journal of Heat and Fluid Flow*, Vol. 24, pp.389–398.
- Monaghan, J.J. (1992) 'Smoothed particle hydrodynamics', *Ann. Rev. Astron. Astrophys.*, Vol. 30, pp.543–574.
- Noui-Mehidi, M.N., Blackburn, H., Manasseh, R., Brooks, G. and Rudman, M. (2005) 'An experimental study on floating solids in a liquid bath', *EPD Congress 2005*, Ed. Mark E. Schlesinger, TMS, pp.655–661.
- Potapov, A.V., Hunt, M.L. and Campbell, C.S. (2001) 'Liquid–solid flows using smoothed particle hydrodynamics and the discrete element method', *Powder Technology*, Vol. 116, pp.204–213.
- Yamazaki, H., Tojo, K. and Miyanami, K. (1991) 'Effect of power consumption on solids concentration profiles in a slurry mixing tank', *Powder Technology*, Vol. 64, pp.199–206.
- Zhu, Y. and Fox, P.J. (2002) 'Simulation of pore-scale dispersion in periodic porous media using smoothed particle hydrodynamics', *J. Comput. Physics*, Vol. 182, pp.622–645.